

Manufacturing of 57cm Carbon-Carbon Composite Ion Optics for the NEXIS Ion Engine

John S. Beatty* and John Steven Snyder†
Jet Propulsion Laboratory, Pasadena, CA, 91109-8099

Wei Shih‡
Allcomp Inc., City of Industry, CA, 91746

Exploration of the outer planets can be taxing on the ion optics of ion propulsion systems because of the higher power and propellant throughput than the present state-of-the art. Carbon-carbon composite ion optics are an enabling technology extending the life of ion optics operated at high specific impulse, power, and propellant throughput because of their low erosion rates compared to molybdenum ion optics. Large 57cm carbon-carbon composite ion optics have been designed, built, and demonstrated for this purpose. Experience and lessons learned from previous developments have led to the successful development of the NEXIS Ion Optics in one design cycle. Ultrasonic inspection of the first set of accelerator grid laminates uncovered intraply delaminations which were resolved in the second set by using an improved laminate cure cycle to liberate more volatiles from the phenolic laminate. Improved control of carbon-carbon manufacturing processes has resulted in grids with open area fraction control to within $\pm 0.6\%$ of design. Completed NEXIS ion optics assemblies have demonstrated aperture alignment better than 0.13 mm and grid gap control to better than 5% across the entire 57-cm-dia. active area of the grids. The design and manufacturing methods used in the production of the NEXIS carbon-carbon ion optics have been validated not only by these assembly inspections, but by the successful completion of NEXIS engine performance and vibration testing.

I. Introduction

THE NEXIS Ion Engine relies on carbon-carbon (CC) composite ion optics for long life. The NEXIS engine^{1,2} can provide specific impulse of 7500s, thruster power over 20kW, and propellant throughput greater than 2000kg using carbon-carbon composite as a major technology enabler. These carbon grids provide a factor of 8-9.5 improvement in life compared to grids made from molybdenum³⁻⁵. The very low sputter erosion rate, high material stiffness, and low coefficient of thermal expansion of carbon-carbon composite materials make this material ideal for ion optics structures.

Grids built from CC are certainly not new for smaller ion engines⁶⁻⁸. Carbon-carbon composite optics have recently been flown on the Hayabusa mission⁹. The Carbon-Based Ion Optics (CBIO) project¹⁰⁻¹² demonstrated that 30cm CC ion optics can be built at a reasonable cost, operated with good performance, and survive launch loads. The larger size of the NEXIS Ion engine challenged us to take the CC production process to an entirely new scale. The NEXIS Optics have an overall size of 77cm with a 57cm diameter beam, roughly twice the size of the CBIO optics. The lessons learned from CBIO provided a very valuable starting point, but many challenges had to be overcome in order to successfully demonstrate the NEXIS 57cm ion optics. These lessons, combined with special attention to design improvements, have enabled us to build launch-survivable ion optics with long life and good performance.

* Staff Engineer, Materials Testing & Contamination Control Group, AIAA Member.

† Member of the Technical Staff, Propulsion and Materials Section, AIAA Member.

‡ Engineer, AIAA Member

This paper discusses the successful production of the NEXIS carbon-carbon ion optics assembly and the results of material and dimensional inspections. Two optics assemblies have been subjected to testing on the NEXIS ion engine and those results are reported elsewhere. In one test¹³ the ion engine met all of its performance goals and is presently undergoing a wear test. In a separate test, the thruster (including the ion optics assembly) successfully withstood protoflight vibration testing¹⁴. Although material quality and dimensional control are important, the successful engine performance and vibration tests are the ultimate indication of the success of the ion optics design and fabrication.

II. Ion Optics Assembly Overview

The design of the optics structure follows the form successfully demonstrated by the CBIO optics. Both the Screen and Accelerator Grids have a spherical shape to provide additional stiffness to resist launch vibration. The grid radii are selected to create a uniform gap between the Screen Grid and Accelerator Grid domes when assembled.

The Screen grid is bonded into a carbon-carbon composite structure to provide greater stiffness (Figure 1). Large holes are included in the edge of the Screen Grid to allow inspection of the interior of the box structure of the Screen Assembly. The Screen-to-Accelerator Grid Insulator Assemblies are installed in the box cavities shown at the edge of the assembly in Figure 2. These box cavities provide additional shadow shielding to protect the grid insulators from sputtered carbon.

Special measures were taken to design an optics assembly which is easy to build and service. The most important improvement was the creation of alignment features to assist in assembly of the Screen and Accelerator Grid apertures. Previous efforts have required lengthy manual alignment procedures to achieve the desired aperture alignment. The alignment features allow for proper orientation of the Screen Grid in the Screen Assembly stiffening structure during bonding. The same alignment features are used for quick and repeatable location of the Accelerator Grid relative to the Screen Grid upon assembly. The process of adjustment of the gap between the Screen and Accelerator grid requires several cycles of assembly and disassembly, so the time-saving benefits of alignment features quickly add up. This ease of assembly allows us to quickly adjust grid gap to within 5% of the target value across the entire area of the optics

The NEXIS ion optics were designed to allow for optics installation as an integrated assembly. This allows us to optimize and lock the grid gap once prior to engine assembly. Subsequent engine disassembly and reassembly has no effect on optics alignment or grid gap.

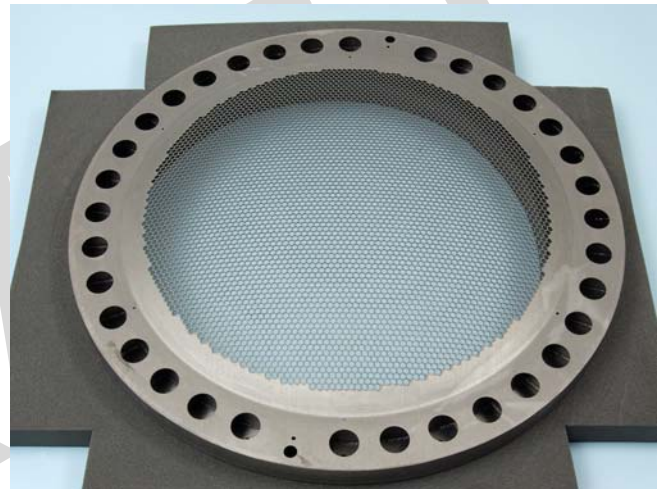


Figure 1: NEXIS Screen Grid Assembly

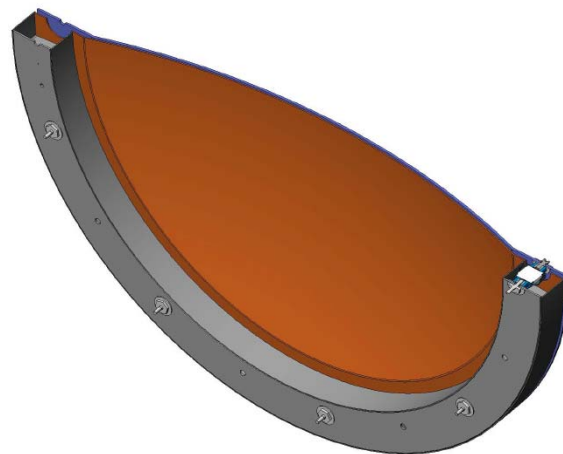


Figure 2: Cross Section of Screen Assembly Model

We developed a new algorithm for locating the roughly 5000 holes in the active area of the grid to better achieve a hexagonally-symmetric hole pattern. Previous algorithms used calculations in a mathematical matrix based on orthogonal (XY) axes for calculation of hole centerpoints. The method of calculation has impact on the symmetry of the hole pattern. The new algorithm improves upon previous work and creates grids with 3 axes of symmetry.

III. CC Materials & Production Processes

The materials used in construction of the NEXIS Ion Optics make the best use of critical material properties while keeping material costs as low as possible. The Screen and Accelerator Grids are built as a laminate of P30X unidirectional fiber in a carbonized phenolic matrix. The flexible and inexpensive pitch-based P30X fiber is easier to work with and much less expensive than premium high-modulus fiber, yet can reach an elastic modulus greater than 690GPa after high-temperature heat treatment.

While the Screen and Accelerator Grids require extremely high elastic modulus in order to survive launch vibration, the other carbon-carbon structures in the Screen Grid assembly can be built from standard inexpensive carbon-fiber laminates. The ring-shaped box structure and flat mounting ring are built from woven fabric of T300 carbon fiber in a carbonized phenolic matrix.

The production process for carbon-carbon composite ion engine grids is lengthy and involves several steps, but is also predictable and repeatable. The processing steps are:

1. Order custom-made prepreg materials
We use custom-designed prepreg in order to build laminates with precisely the right thickness for proper operation of the ion optics. Phenolic resin is chosen for the best carbon char yield and cure performance. Prepreg resin content is specified by considering final target fiber content and the percentage of mass lost during processing.
2. Fabrication of graphite layup tools
The graphite layup tools control the shape of the carbon-phenolic laminate, which in turn determines the shape of the completed grids. Graphite is the material of choice because of the low coefficient of thermal expansion and high usage temperature. The NEXIS tooling consists of a concave and nested convex mold to control both the inside and outside surface smoothness and radius of curvature. Separate tools are used for the Screen and Accelerator grids. The high usage temperature is necessary because of the high-temperature carbonization and graphitization processing steps. The specific variety of graphite is selected to minimize cost while providing low porosity, small grain size, and isotropic material properties.
3. Construction of carbon-phenolic laminate
Once the mold is complete, the basic carbon-phenolic laminate can be built in the same manner as any typical carbon-phenolic structural laminate. Alternating layers of unidirectional fiber prepreg are placed on the tool and compacted to yield a laminate with symmetric ply orientation about the centerline of the laminate thickness. The 2-part concave-convex mold design allows for laminate curing in a heated press without need for an autoclave.
4. Carbonization
The phenolic matrix holding the laminate fibers together is reduced to pure carbon by high-temperature firing in an oxygen-free atmosphere. This carbonization process drastically reduces the strength and mass of the laminate, requiring densification to raise density and structural integrity.
5. Densification by Chemical Vapor Deposition / Infiltration
Additional carbon is added to the laminate matrix through Chemical Vapor Deposition. In this lengthy process, the carbonized laminates are processed for up to 200 hours in a vacuum at high temperature in the presence of carbon-bearing gas. The gas is cracked liberating hydrogen while carbon is deposited on the surface and in the microvoids of the porous laminate. This increases

the density and strength of the carbon-carbon laminate. Inspection is performed after densification to check part dimensions and density.

6. Graphitization Heat Treatment (for grids only)

Graphitization of the Screen and Accelerator grids subjects the pitch-based P30X fiber to a structural change through fiber graphitization at very high temperature. At this temperature, the fiber elastic modulus is dramatically increased while the fibers grow in length. The heat treatment imparts the laminate fibers with the stiffness required for the grids to survive launch vibration without collision. Accurate prediction and control of grid dome radius during this step is critical in order to keep grid gaps uniform upon assembly. Inspection is performed after graphitization to check part dimensions and density.

7. Validation of Grid Hole Centerpoint Data

The complex algorithm for design of the Screen and Accelerator Grid hole pattern must be validated to insure the instructions for laser machining are correct. The use of 3D modeling of the hole centerpoints can verify that the algorithm parameters are correct. This validation step includes a design review and documentation of the grid design parameters and expected open area fraction for both grids.

8. Laser Machining

Laser machining is the preferred method¹⁵⁻¹⁷ for cutting the grid features in the grid blanks. Hole centerlines are coaxial on a line originating from the centerpoint of the grid spherical dome. The locations of the holes are controlled in a way to allow grids to be interchangeable. Inspection is performed after machining to check the part dimensions and hole location precision.

9. Bonding of Screen Assembly

The three discreet CC parts comprising the Screen Assembly must be bonded with carbon-bearing adhesive to build the stiffened Screen Assembly. Adhesive is carefully placed at joints inside and outside the ring-shaped box structure to restrain both the Screen Grid and flat Mounting Ring. Special care must be taken to properly align the Screen Grid to the Mounting Ring during bonding. The adhesive is carbonized during the final Chemical Vapor Deposition / Infiltration step.

10. Final densification by Chemical Vapor Deposition / Infiltration

The final densification step fills the open voids exposed during machining of thousands of holes during the laser machining process, while carbonizing the Screen Assembly adhesive. This process also applies a surface finish of glassy carbon that increases the voltage standoff of the grid assembly^{18,19}.

11. High-Temperature Vacuum Bakeout

All carbon-carbon structures to be used in ion engines should be subjected to high temperature and low pressure for several hours in order to liberate hydrocarbons and other volatile gases trapped inside the structure of the carbon-carbon composite material. This bakeout process reduces or eliminates the outgassing which would otherwise be encountered when the ion engine is run for the first time.

12. Inspection of Screen Assembly and Accelerator Grid

The completed Screen Assembly and Accelerator Grid are inspected using a coordinate-measuring machine to evaluate the finished products.

13. Optics Assembly, Gap Adjustment, and Inspection

The optics must be assembled with shims for proper adjustment of the gap between the Screen and Accelerator Grid. Measurements are taken to assess hole diameters, alignment, and grid gap.

IV. Production Optimization

A. Mold Design

Proper design of the Screen Grid and Accelerator Grid molds is essential to obtain the correct optics grid gap. In order to get the correct grid gap across the entire span of the active area of the optics, both the Screen and Accelerator grid dome radii of curvature must be tightly controlled. The prediction of the completed dimensions of typical composite structures can usually be calculated knowing the dimensions of the mold and coefficient of thermal expansion of the mold material. This is not necessarily true for carbon-carbon composites. Carbon-carbon structures experience dimensional changes during the high-temperature graphitization process. Inspection data from previous grid fabrications showed growth in the radius of curvature to be 1.3%. The NEXIS molds were designed to account for 1.3% growth, but as the data in Table 2 and Table 1 shows, the radius of curvature increase was slightly less for Screen Grid SN003 and Accelerator Grid SN001.



Figure 3: 3D Model of NEXIS Optics Layup Tool

Table 2: Dome Radius Change for NEXIS Screen Assembly

Screen Assembly, Serial No. 003	
Predicted Radius Change	1.3%
Actual Radius Change	1.1%
Deviation	0.2%
Measured Surface Variation	± 0.042 mm

Table 1: Dome Radius Change for NEXIS Accelerator Grid

Accel Grid Serial No. 001	
Predicted Radius Change	1.3%
Actual Radius Change	0.9%
Deviation	0.5%
Measured Surface Variation	± 0.092 mm

B. Porosity Mitigation

A major challenge in the production of NEXIS Ion Optics was mitigation of porosity and delaminations. Ultrasonograph inspection of the Screen and Accelerator grids after the first densification cycle revealed delaminations in the thicker Accelerator grids. Delaminations are apparent as black regions in the scan shown in Figure 4. The thinner Screen grids had no delaminations, as shown in Figure 5.

The presence of intralaminar trapped gases was identified as a probable cause for the observed delaminations. Phenolic resins, such as those used in the NEXIS grids, are known to produce large quantities of water vapor which

can easily be trapped in the form of pores and voids. Curing of the laminate pressed between two solid molds only makes the problem worse as all volatiles must exit the mold by traveling within the layers of the laminate during the cure process. The larger diameter of the NEXIS optics increases the distance trapped gases must travel to exit the 80cm diameter mold. These trapped volatiles can expand during high-temperature processing and are likely the primary cause of delaminations in the NEXIS Accelerator Grid.

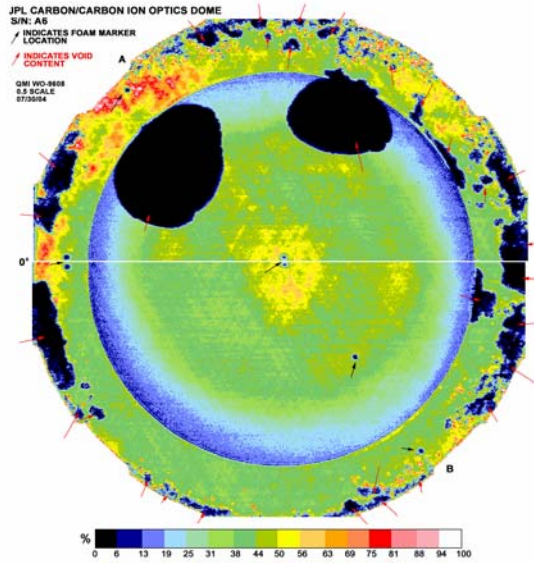


Figure 4: Ultrasonograph of thick NEXIS Accelerator Grid prior to machining: Delaminations are indicated in solid black areas.

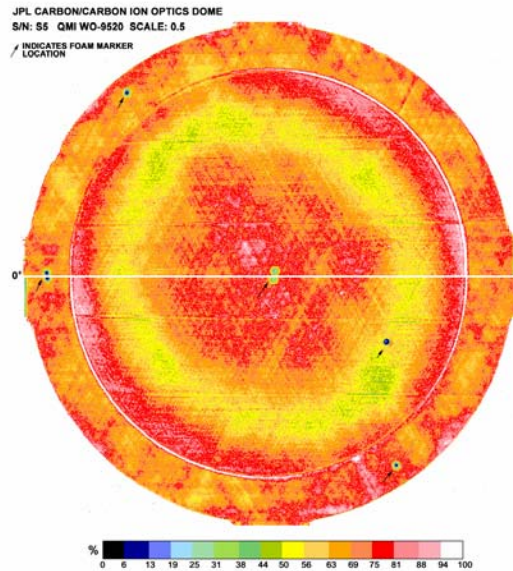


Figure 5: Ultrasonograph of thin NEXIS Screen Grid prior to machining: No detectable porosity or delaminations

While all of the delaminations were easily detected by ultrasonic inspection, the large black areas on the ultrasonograph were also often visible by visual inspection as slight bulges in the surface profile of the grids. While some porosity may be acceptable, these large delaminations can cause noticeable changes in the surface profile of the grids, and are thus not acceptable. Any cause for variability in the surface profile will have effects on the uniformity of the optics grid gap. To eliminate the delaminations, the laminate cure cycle was extended to lengthen the time at the low and intermediate temperatures. The modified cure cycle was also conducted under vacuum to further assist in removal of trapped volatiles.

The success of the modified cure cycle is illustrated by the ultrasonograph shown in Figure 6, where the large areas of delaminations are no longer observed. While some porosity may still be present, the serious delaminations are gone. The remaining porosity is mitigated during the final CVD process.

The red coloration of the Screen Grid ultrasonograph is a result of lower sound attenuation associated with the thinner Screen Grid material and should not be considered positive indication of porosity throughout the laminate.

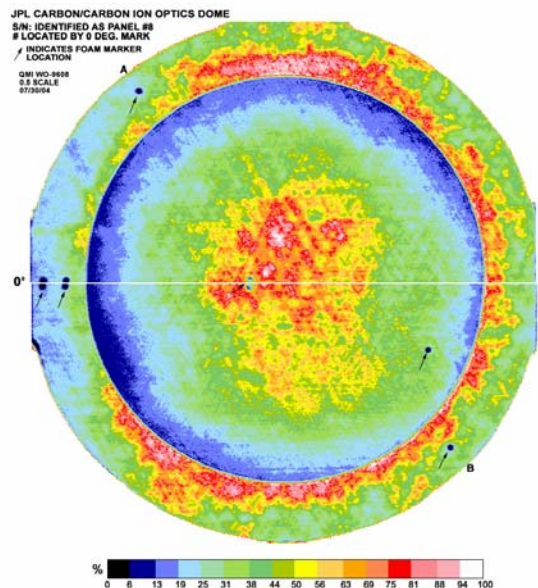


Figure 6: Ultrasonograph of unmachined NEXIS Accelerator Grid prior to machining: Cure cycle modifications eliminated delaminations.

C. Hole Pattern Design & Machining

Specification of the exact centerpoints of the thousands of grid holes is a challenging task. The design requirements for uniform hole spacing on a spherical surface pose what seem to be contradictory requirements. It may not be immediately obvious that a perfectly-periodic hexagonal pattern cannot be projected onto a spherical surface. Compromises are necessary. The NEXIS Optics hole pattern design objectives were chosen to control the design parameters important to performance while allowing necessary variability in other parameters. The main design objective is to design functional grids that are completely interchangeable and can be properly oriented in all six possible Accelerator Grid orientations. The algorithm was designed to allow this while keeping open area fraction as uniform as possible in the center of the optics.

The requirement for interchangeability and assembly orientation flexibility was the reason that a new hole calculation algorithm was developed to use non-orthogonal axes. This algorithm calculates the hole centerpoints for a 60° “wedge” of both the Screen and Accelerator grid. This collection of hole centerpoints can be duplicated and rotated through five coordinate transformations to create the hole pattern for the remaining 300° of the grid pattern. The use of non-orthogonal axes with 60° separation (Figure 7) makes the calculation easier and ensures that the duplicated and rotated wedge regions have proper hole repetition at the boundaries between each wedge. This calculation method guarantees that the grids can be assembled and aligned in six different ways while still preserving simultaneous alignment of the entire hole pattern.

Since the holes are to be placed on a spherical surface, the algorithm controls the arc length rather than straight-line distance between holes. The holes located on the R and S axes are spaced at constant arc length intervals. This constant hole spacing along the “spokes” of the R and S axes is what creates the distinctive star-shaped pattern of uniform open area fraction in six radial spokes as seen in Figure 9. The arc-length spacing between holes is most distorted for holes located furthest from the R and S axes. The total variation in local open area fraction in the Screen Grid is $\pm 0.6\%$, with the highest open area fraction occurring in the center and along the spokes of the duplicated R-S axes.

The orientation of the hole pattern relative to the laminate fiber orientation is controlled to preserve continuous fibers as much as possible. The laminate fiber orientation $[0, +60, -60, -60, +60, 0]_{ns}$ is perfectly suited for compatibility with the hexagonal hole pattern as shown in Figure 8.

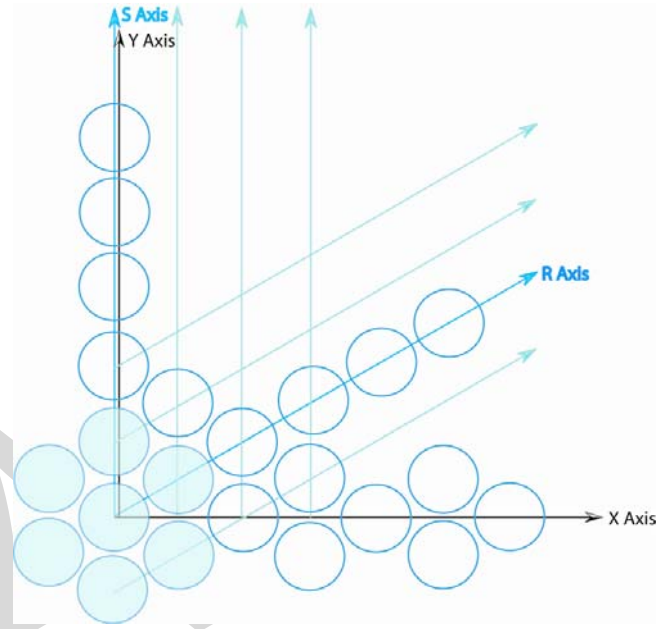


Figure 7: Non-orthogonal axes used for creation of grid hole pattern

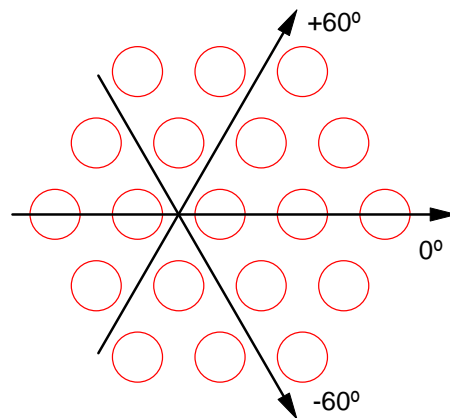


Figure 8: Laminate Fiber Orientation Relative to Hole Pattern

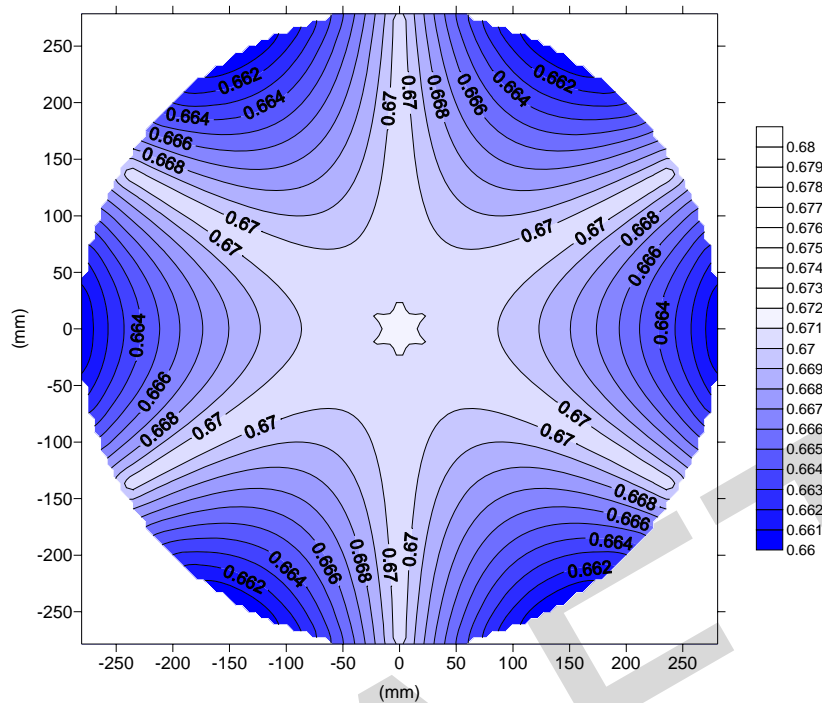


Figure 9: Plot of Screen Grid Nominal Open Area Fraction: *Variations in open area fraction are minimized.*

V. Inspection of Completed Assembly

The grid alignment, hole diameters, and grid gap were all measured using a coordinate measuring machine. A quantity of 19 hole pairs were selected at 6 azimuths and 3 evenly-spaced distances from the optics centerline as shown in Figure 11.

Inspection of Screen and Accelerator Grid hole diameters shows very precise control of hole diameter during manufacturing. Inspection verifies that the laser-cut holes, as shown in Figure 10, consistently have uniform round boundaries free of sharp edges. Hole diameters were measured (Figure 12 and Figure 13) using a coordinate measuring machine making twelve contact measurements per hole. The Accelerator Grid hole diameters are measured with the CMM probe passing through the Screen Grid hole, making visual guidance of the CMM more difficult and increasing measurement error.



Figure 10: Micrograph of Screen Grid Hole

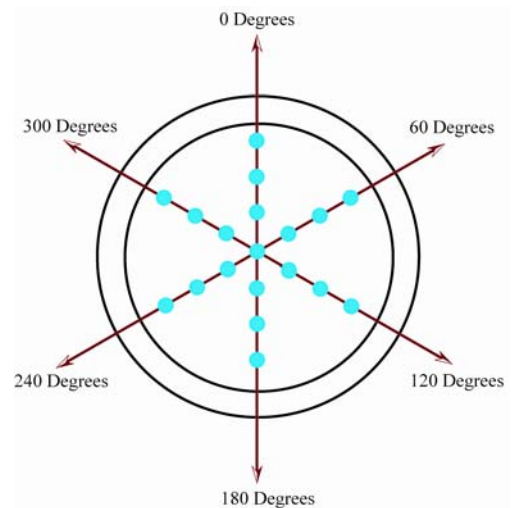


Figure 11: Measurement Locations for Hole & Gap Inspection

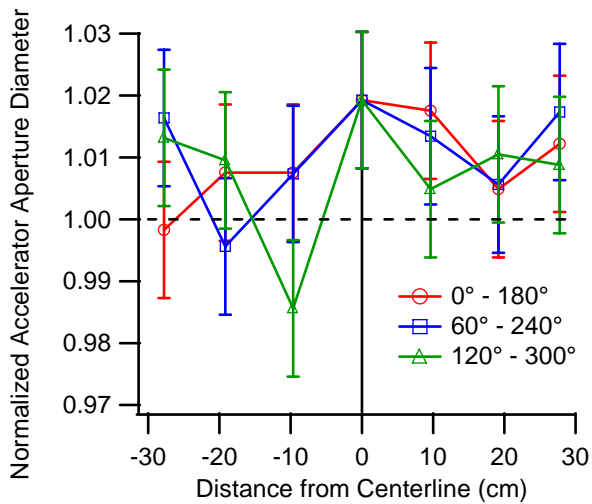


Figure 13: Accel Grid Hole Diameter Deviation

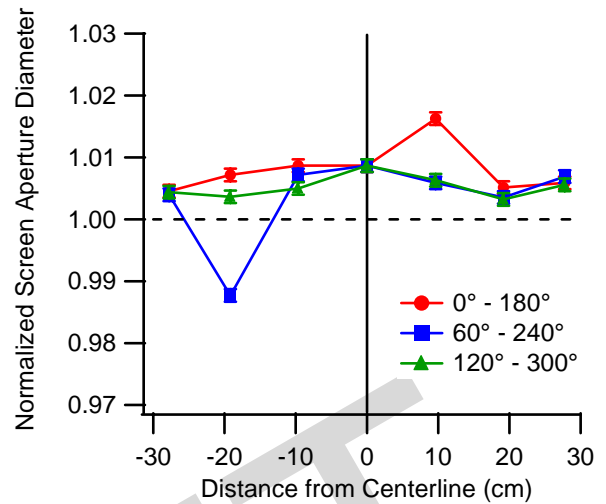


Figure 12: Screen Grid Hole Diameter Deviation

The aperture diameter accuracy directly affects the local open area fraction of the completed grids. The local open area fraction is calculated by considering the nominal distance between hole centerpoints and the measured average hole diameter. The area (A) of a triangle between 3 adjacent holes can be calculated²⁰ knowing the 3 distances (a,b,c) between the 3 hole centerpoints and finding the semi-perimeter (s). Since the sum of the interior angles of the triangle is 180° and each vertex is located at the centerpoint of a hole, each triangle contains 1/2 the area of one hole. Figure 14 and Figure 15 illustrate that the open area fraction is uniform within ±0.6% across the entire active area of the Screen Grid and ±0.25% across the active area of the Accelerator Grid.

$$s = \frac{1}{2}(a + b + c)$$

$$A = \sqrt{s(s - a)(s - b)(s - c)}$$

$$OAF = \frac{HoleArea}{2A}$$

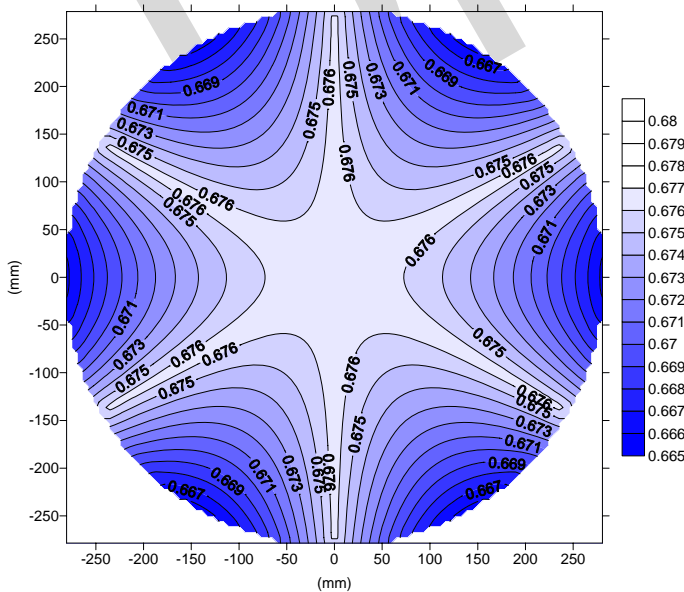


Figure 14: Screen Grid Local Open Area Fraction Based on Average Measured Hole Diameter

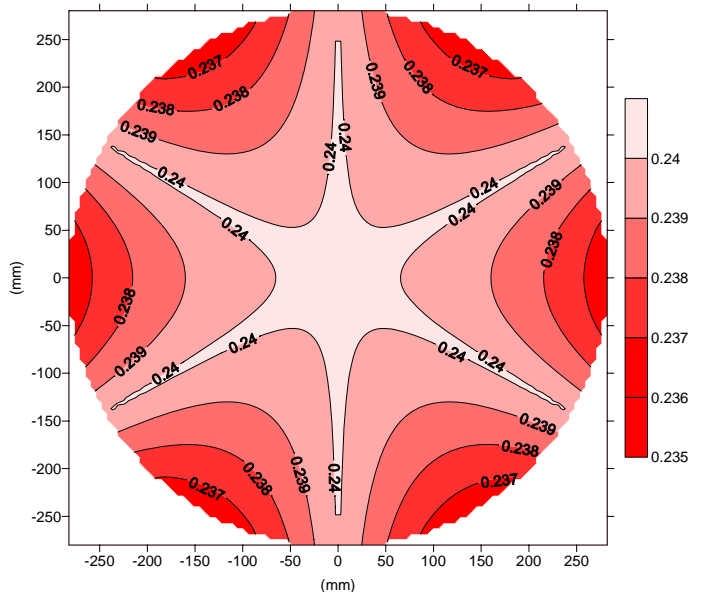


Figure 15: Accel. Grid Local Open Area Fraction Based on Average Measured Hole Diameter

An important measure of success in production of the optics is alignment of hole pairs (Figure 16). Hole centerpoints were measured for matched pairs of holes in the Screen and Accelerator Grids in the assembled state. Inspection results show generally greater alignment deviation near the edge of the grids, but the magnitude of deviation is under 0.13mm across the entire grid active area.

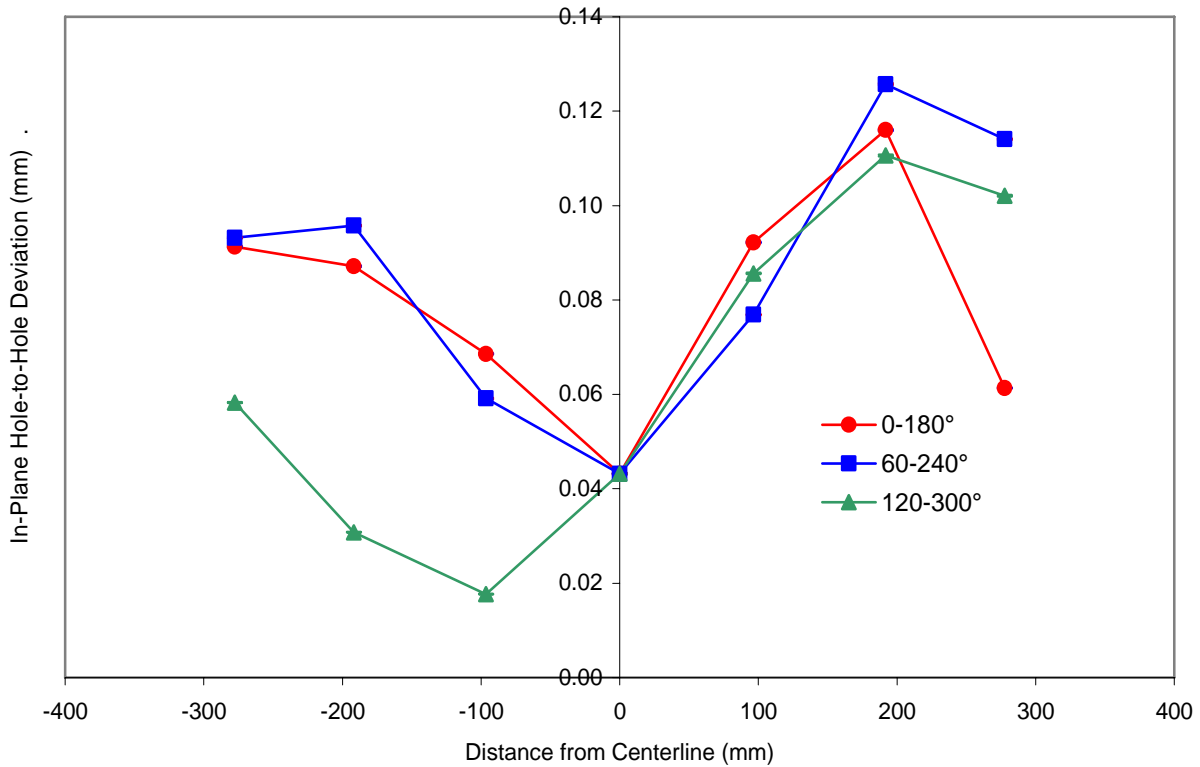


Figure 16: Measured Alignment of NEXIS Ion Optics Hole Pairs

Grid gap was measured by first measuring the centerpoint of the Screen and Accelerator holes at the dome inner surface. It can be seen that using the NEXIS design, materials, and processes, control of the grid gap within better than $\pm 5\%$ was achievable over the entire span of the optics.

Table 3: NEXIS Optics Gap Measurements Summary

	Gap
Target Gap (normalized)	1.000
Measured Values: (normalized)	
Average	1.005
Maximum	1.047
Minimum	0.951
Range	0.096
Standard Deviation	0.034
Number of holes measured	19

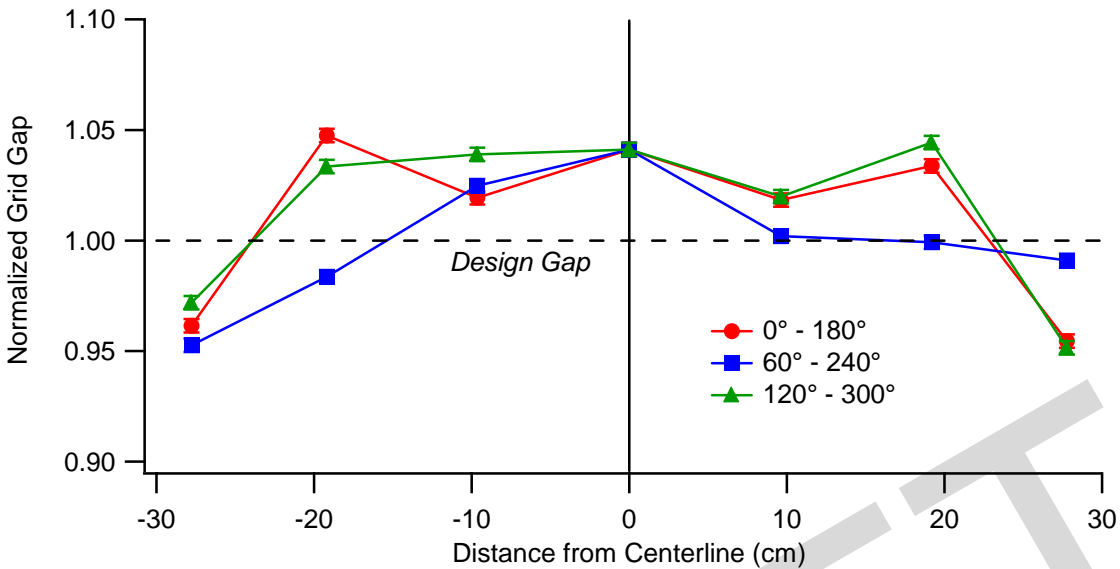


Figure 17: Measured Assembly Grid Gap

VI. Conclusion

The successful production of the NEXIS carbon-carbon composite ion optics demonstrates that the fabrication process is well understood and that the design and manufacturing methods are sufficiently mature to produce flight-quality hardware. Large-diameter carbon-carbon ion optics have been designed and built with grid alignment, hole diameter control, and grid gap control within tight tolerances that meet or exceed the design requirements. The manufacturing knowledge and technology have reached a level to allow successful design and construction during the first design cycle. Although the production of the NEXIS ion optics to design specifications has been demonstrated, the successful engine performance and vibration tests are the ultimate indication of the success of the ion optics design and manufacturing process.

Acknowledgments

The authors would like to recognize the contributions of Mr. Ron Sanders and the team at Southwestern Laser for the high-quality and fast laser machining of NEXIS grids.

This research was carried out at the Jet Propulsion Laboratory, California Institute of Technology, under a contract with the National Aeronautics and Space Administration in support of Project Prometheus.

References

- ¹Randolph, T.M., Polk, J.E., "An Overview of the Nuclear Electric Xenon Ion System (NEXIS) Activity," AIAA 2004-3450, 40th AIAA/ASME/SAE/ASEE Joint Propulsion Conference and Exhibit, Fort Lauderdale, FL, 11-14 July 2004.
- ²Polk, J.E., et al, "An Overview of the Nuclear Electric Xenon Ion System (NEXIS) Program," AIAA 2003-4713, 39th AIAA/ASME/SAE/ASEE Joint Propulsion Conference and Exhibit, Huntsville AL, 20-23 July 2003.
- ³Williams, J.D., Johnson, M.L., Williams, D.D., "Differential Sputtering Behavior of Pyrolytic Graphite and Carbon-Carbon Composite Under Xenon Bombardment," AIAA 2004-3788, 40th AIAA/ASME/SAE/ASEE Joint Propulsion Conference and Exhibit, Fort Lauderdale, FL, 11-14 July 2004.
- ⁴Deltschew, R., et al, "Sputter Characteristics of Carbon-Carbon Compound Material," IEPC 01-118, 27th International Electric Propulsion Conference, Pasadena CA, 15-19 October 2001.
- ⁵Meserole, J.S. "Erosion Resistance of Carbon-Carbon Ion Optics," *Journal of Propulsion and Power*, Vol. 17, No. 1, January-February 2001, pp. 12-18.
- ⁶Garner, C.E., Brophy, J.R., "Fabrication and Testing of Carbon-Carbon Grids for Ion Optics," AIAA 92-3149, 28th AIAA/ASME/SAE/ASEE Joint Propulsion Conference and Exhibit, Nashville TN, 6-8 July 1992.

⁷Mueller, J., Brophy, J.R., Brown, K.D., Garner, C.E., "Performance Characterization of 15-cm Carbon-Carbon Composite Grids," AIAA 94-3118, 30th AIAA/ASME/SAE/ASEE Joint Propulsion Conference and Exhibit, Indianapolis IN, 27-29 June 1994.

⁸Funaki, I., et al, "Verification Tests of Carbon-Carbon Composite Grids for Microwave Discharge Ion Thruster," *Journal of Propulsion and Power*, Vol. 18, No. 1, January-February 2002, pp. 169-175.

⁹Kuninaka, H., Nishiyama, K., Shimuzu, Y., Toki, K., "Flight Status of Cathode-Less Microwave Discharge Ion Engines Onboard HAYABUSA Asteroid Explorer," AIAA 2004-3438, 40th AIAA/ASME/SAE/ASEE Joint Propulsion Conference and Exhibit, Fort Lauderdale, FL, 11-14 July 2004.

¹⁰Snyder, J.S., Brophy, J.R., "Performance Characterization and Vibration Testing of 30-cm Carbon-Carbon Ion Optics," AIAA 2004-3959, 40th AIAA/ASME/SAE/ASEE Joint Propulsion Conference and Exhibit, Fort Lauderdale, FL, 11-14 July 2004.

¹¹Snyder, J.S., Brophy, J.R., Goebel, D.M., Beatty, J.S., De Pano, M.K., "Development and Testing of Carbon-Based Ion Optics for 30cm Ion Thrusters," AIAA 2003-4716, 39th AIAA/ASME/SAE/ASEE Joint Propulsion Conference and Exhibit, Huntsville AL, 20-23 July 2003.

¹²Snyder, J.S., "Review of Carbon-Based Grid Development Activities for Ion Thrusters," AIAA 2003-4715, 39th AIAA/ASME/SAE/ASEE Joint Propulsion Conference and Exhibit, Huntsville AL, 20-23 July 2003.

¹³Polk, J.E., Goebel, D.M., Snyder, J.S., Schneider, A.C., Sengupta, A., "NEXIS Ion Thruster Performance and Wear Test Results," AIAA 2005-4394, to be presented at 41st AIAA/ASME/SAE/ASEE Joint Propulsion Conference and Exhibit, Tucson, AZ, 10-13 July 2005.

¹⁴Snyder, J.S., et al., "Vibration Test and Analysis of the NEXIS Ion Engine," AIAA 2005-4412, to be presented at 41st AIAA/ASME/SAE/ASEE Joint Propulsion Conference and Exhibit, Tucson, AZ, 10-13 July 2005.

¹⁵Mueller, J., Brophy, J.R., Brown, D.K., "Endurance Testing and Fabrication of Advanced 15cm and 30cm Carbon-Carbon Composite Grids," AIAA 95-2660, 31st AIAA/ASME/SAE/ASEE Joint Propulsion Conference and Exhibit, San Diego CA, 10-12 July 1995.

¹⁶Brophy, J.R., Mueller, J., Brown, D.K., "Carbon-Carbon Ion Engine Grids with Non-Circular Apertures," AIAA 95-2662, 31st AIAA/ASME/SAE/ASEE Joint Propulsion Conference and Exhibit, San Diego CA, 10-12 July 1995.

¹⁷Mueller, J., Brophy, J.R., Brown, D.K., "Design, Fabrication and Testing of 30cm Dia. Dished Carbon-Carbon Ion Engine Grids," AIAA 96-3204, 32nd AIAA/ASME/SAE/ASEE Joint Propulsion Conference and Exhibit, Lake Buena Vista, FL, 1-3 July 1996.

¹⁸Goebel, D.M., Schneider, A.C., "High Voltage Breakdown and Conditioning of Carbon and Molybdenum Electrodes," to be published in IEEE Transactions on Plasma Science, August 2005.

¹⁹Goebel, D.M., "High Voltage Breakdown Limits of Molybdenum and Carbon-based Grids for Ion Thrusters," AIAA 2005-4257, to be presented at 41st AIAA/ASME/SAE/ASEE Joint Propulsion Conference and Exhibit, Tucson, AZ, 10-13 July 2005.

²⁰Zwillinger, D. (ed), *CRC Standard Mathematical Tables and Formulae*, 31st ed., Chapman & Hall / CRC, Boca Raton, 2003, pp. 319.